Ice Transit and Performance Analysis for Cryorobotic Subglacial Access Missions on Earth and Europa

Marc S. Boxberg[1], Qian Chen[1], Ana-Catalina Plesa[2], and Julia Kowalski[1]

[1]Chair of Methods for Model-based Development in Computational Engineering, RWTH Aachen University, Aachen, Germany, [2]Institute of Planetary Research, German Aerospace Center (DLR), Berlin, Germany – E-Mail: boxberg@mbd.rwth-aachen.de

1. Introduction

It is widely recognised that the icy moons of our solar system are interesting candidates for the search for habitable environments beyond Earth. While upcoming space missions such as the Europa Clipper and JUICE missions will give us further insight into the local cryo-environment of Jupiter's moon Europa, any conclusive survey to detect life will require the ability to penetrate and traverse the ice shell and access the subglacial ocean directly. Developing a robust, autonomous cryobot for such a mission is an extremely demanding challenge and requires a concentrated interdisciplinary effort by engineers, geoscientists and astrobiologists.

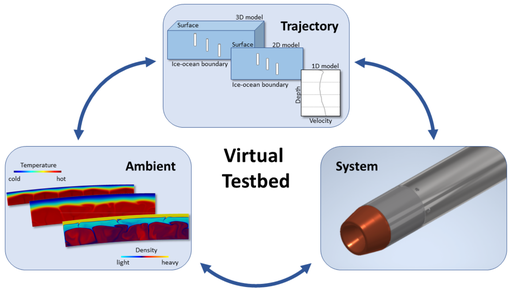

▲ **Fig. 1:** Schematic sketch of the virtual testbed approach. It consists of a description of the system, that is, the cryobot, the ambient, for example, ice properties, and the calculated trajectory. As an example for a cryobot/system, the EnEx-RANGE APU is shown (Weinstock et al., 2020). The description of the ambient and the trajectory have multiple levels of detail. For the ambient, a basic layer might consist of a homogeneous description of the ice; further levels include more detail like salt distributions of increasing complexity or dust within the ice. Similarly, the trajectory modeling can have different complexity from simple performance models to full 3D high-fidelity finite element models.

2. Mission Scenarios to Be Analyzed

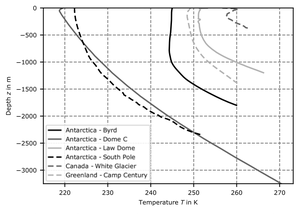

◀ **Fig. 2:** Observed temperature profiles for six terrestrial deployment scenarios in Antarctica, Canada, and Greenland.

▼ **Fig. 3:** Variations of temperature (left) and density (right) in the ice shell of Europa as obtained from a geodynamical model. The model assumes an ice shell thickness of 40 km and a maximum density contrast due to salts of 23 kg/m³. The colorbar for the density is saturated at 922 kg/m³ to show density variations within the ice shell. The snapshots show the distribution of temperature and density after 3.8 Ma when the simulation reached a statistical steady state.

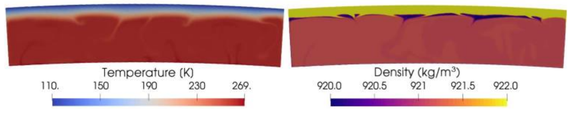

3. Computational Trajectory Prediction

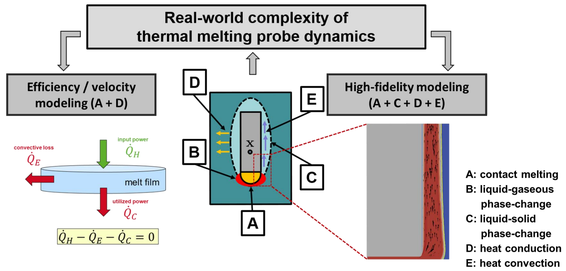

▲ **Fig. 4:** The forward motion of an ice melting probe is a complex multi-physics problem involving several processes, such as contact melting (A), vaporization (B), melting (C), heat conduction (D), and heat convection (E). To approach the real-world complexity of the model there are two main modeling options available: high-fidelity modeling that solves the coupled problem numerically for temperature distribution, fluid velocity and phase interfaces on a computational grid or semi-analytical efficiency / velocity modeling that solves the energy balance to obtain the melting velocity. We consider the latter approach in this work.

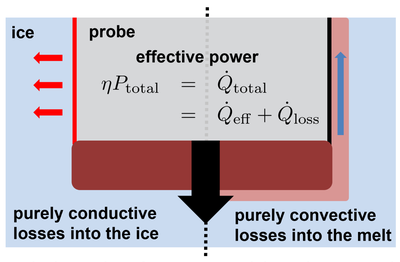

▲ **Fig. 5:** Velocity and performance models estimate to which part the thermal melting probe's total available rate of heat flow Q_{total} is leveraged for forward motion Q_{eff}. Two conceptually different approaches exist that either neglect the melt water around the probe and assume that heat is dominantly lost by direct lateral conduction into the ice (left side of the symmetry axis), or alternatively that account for the melt water and assume heat loss to be due to convective transport with the melt water (right side of the symmetry axis).

Simplest assumption: all heat provided by the melting probe is leveraged for forward motion (Aamot, 1967)

$$\dot{Q}_{\text{eff}} = \dot{Q}_{\text{latent}} + \dot{Q}_{\text{sensible}} = VA\rho_{\text{i}}L + VA\rho_{\text{i}}c_{\text{p,i}}\left(T_{\text{m}} - T_{\text{i}}\right)$$

More realistic: the ice is not directly heated, but the microscale melt film, so convective losses can occur; CCM (Schüller & Kowalski, 2019)

$$\dot{Q}_{\text{total}} = \dot{Q}_{\text{latent}} + \dot{Q}_{\text{sensible}} + \dot{Q}_{\text{convective}} = \gamma\left(\dot{Q}_{\text{latent}} + \dot{Q}_{\text{sensible}}\right)$$

$$\gamma = \frac{1-3D}{7D+1}, D = \frac{1}{20\alpha}\left(\frac{\rho_{\text{i}}}{\rho_{\text{w}}}VR\right)^{4/3}\left(\frac{3\pi\mu_{\text{w}}}{2F^*}\right)^{1/3}$$

Trajectories can be integrated from both approaches:

Velocity V can numerically be determined from the energy balance and be integrated into a global trajectory (Boxberg et al., 2023):

$$z(t) = \int_0^t V\left(P_{\text{total}}(\tau), T_{\text{i}}\left(z(\tau)\right), c_{\text{p,i}}\left(T_{\text{i}}\left(z(\tau)\right), \dots\right), \dots\right)\mathrm{d}\tau$$

4. Results

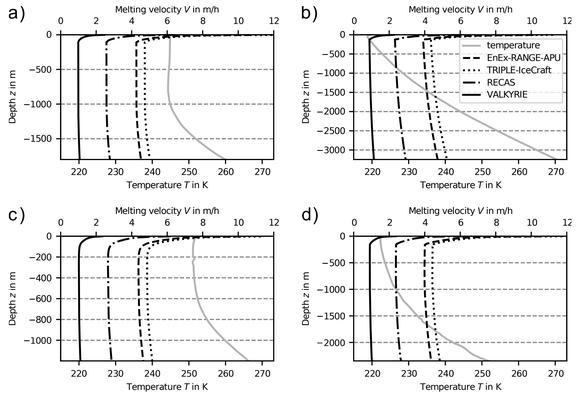

▲ **Fig. 6:** Trajectories in terms of the melting velocity as a function of the depth and temperature profiles for the terrestrial scenarios: (**a**) Antarctica—Byrd, (**b**) Antarctica—Dome C, (**c**) Antarctica—Law Dome, (**d**) Antarctica—South Pole. The temperature is plotted as a solid gray line and the trajectories of the four considered cryobots are plotted as black lines. Note that the legend in (**b**) is valid for the other subfigures, too.

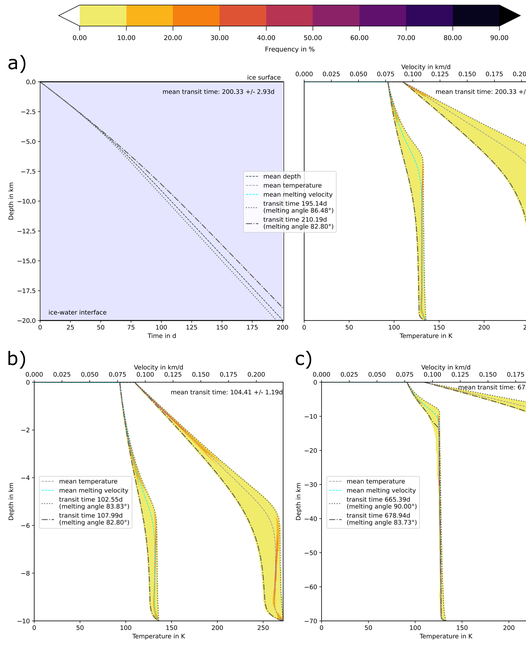

▲ **Fig. 7:** Trajectories for Europa scenarios with ice thicknesses of (**a**) 20 km—transit time (left) as well as velocity and temperature (right) with respect to depth, (**b**) 10 km, and (**c**) 70 km.

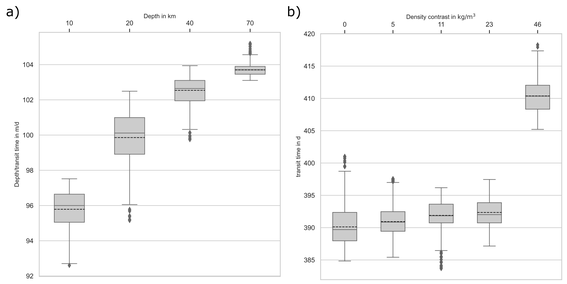

▲ **Fig. 8:** Uncertainties in transit time for the different considered Europa scenarios plotted as box and whisker plots. The lower and upper border of the box are the lower and upper quartile values of the data, with a line at the median. The dashed line within the box is the mean. The range of the data is shown by the whiskers. Outliers are plotted as diamonds outside the ends of the whiskers. (**a**) Average melting velocity over the whole ice thickness is plotted as the ratio of depth and transit time in m/d for different ice thickness and assuming no density contrast. (**b**) Transit time for different density contrasts, including uncertainty in temperature and density profiles, depending on the location of the landing site.

▼ **Fig. 9:** Trajectory for Europa scenarios with an ice thickness of 40 km and varying density contrasts. For each field, that is, time, velocity, and temperature, the frequency of occurrence per depth is plotted color coded according to the given colorbar. In addition, the mean is given by a dashed line.

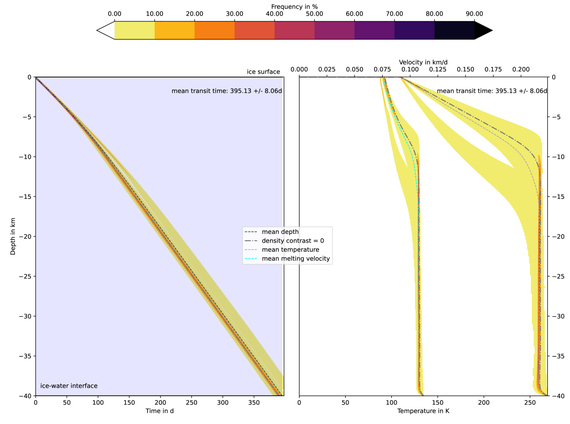

5. Conclusions

We present ice transit and performance models as a first step towards a modular virtual testbed (Fig. 1) for cryorobotic exploration technologies used to investigate the habitability potential of englacial and subglacial environments on icy moons. While we focused on rather idealized models within the scope of this work, future extensions to the virtual testbed will include models of higher complexity and consider non-uniform distributions of salt concentration, which have been observed in terrestrial icy drilling. Furthermore, the effects of additional impurities, such as dust, on the trajectories will be investigated in future studies.

References

Aamot (1967) Heat transfer and performance analysis of a thermal probe for glaciers. CRREL Special Report, U.S. Army Material Command Cold Regions Research and Engineering Laboratory, Hanover, New Hampshire, 119.

Boxberg et al. (2023) Ice Transit and Performance Analysis for Cryorobotic Subglacial Access Missions on Earth and Europa. Astrobiology 23(3)

Schüller and Kowalski (2019) Melting probe technology for subsurface exploration of extraterrestrial ice–critical refreezing length and the role of gravity. Icarus 317:1–9.

Weinstock et al. (2020) The autonomous Pinger unit of the acoustic navigation network in EnEx-range: an autonomous in-ice melting probe with acoustic instrumentation. Ann Glaciol 2020:1–10.

Gefördert durch:
Bundesministerium für Wirtschaft und Energie
aufgrund eines Beschlusses des Deutschen Bundestages
FKZ: 50NA1908

Chair of Methods for Model-based Development in Computational Engineering

RWTH AACHEN UNIVERSITY